Geshi *et al. Earth, Planets and Space* (2022) 74:20
https://doi.org/10.1186/s40623-022-01577-7

Earth, Planets and Space

FULL PAPER Open Access

Evolution of the magma plumbing system of Miyakejima volcano with periodic recharge of basaltic magmas

Nobuo Geshi[1*], Teruki Oikawa[1], Derek J. Weller[2] and Chris E. Conway[1]

Abstract

Defining the variations in petrological characteristics of erupted magmas within a high-resolution chronostratigraphy provides a necessary framework for monitoring the long-term activity and eruption potential of an active volcano. Here, we investigate the evolution of the magmatic system of Miyakejima volcano, Japan, between the last two caldera-forming eruptions, at ~2.3 ka and AD 2000, based on new stratigraphic constraints, radiocarbon ages, and whole-rock geochemical data. The activity of Miyakejima during this interval can be divided into three magmatic periods based on cyclic whole-rock compositional trends. Period 1 spans the interval between ~2.3 ka and the 7th century, from the Hatchodaira eruption with caldera collapse to immediately before the Suoana–Kazahaya eruption. Period 2 spans the time period between the seventh century and the fourteenth century, from the Suoana–Kazahaya to the Sonei–bokujyo eruptions. Period 3 covers the period from the two major flank eruptions that occurred in the sixteenth century to the end of the twentieth century until the last caldera-collapse event in AD 2000. The eruption rate decreased from 0.5 km^3 per 1000 years in Period 1 to ~0.2 km^3 per 1000 years in Period 2 and 3. Recharge of primitive basaltic magmas into shallower crustal systems triggered extensive basaltic fissure eruptions at the beginning of each period. Progressively increasing whole-rock SiO_2 contents of the hybrid magmas in subsequent eruptions indicates continuous fractional crystallization in small shallow magma chambers which formed at the start of each magmatic period. Intermittent injections of basaltic magma into shallow magma chambers induced magma mixing that caused eruption of hybrid basaltic andesite in each period. We suggest that some basaltic magmas formed isolated magma reservoirs at shallow depth, in which rapid fractionation was able to occur. Rupturing of these isolated magma storage regions filled with gas-rich evolved magma can lead to violent ejection of andesitic magmas, such as for the Suoana–Kazahaya eruption in the seventh century. Our results suggest two main scenarios of eruption for the basaltic magma system at Miyakejima and similar mafic volcanoes in the northern Izu–Bonin arc; (1) eruption of voluminous basaltic lavas after the recharge of primitive basaltic magmas into the shallow magmatic system, and (2) explosive fissure eruption by rupturing of isolated magma bodies filled with gas-rich evolved magmas.

Keywords: Volcanic stratigraphy, Magma feeding system, Magma recharge, Mafic volcano, Miyakejima

*Correspondence: geshi-nob@aist.go.jp
[1] Geological Survey of Japan, AIST, AIST Site 7, 1-1-1 Higashi, Tsukuba, Ibaraki, Japan
Full list of author information is available at the end of the article

Graphical Abstract

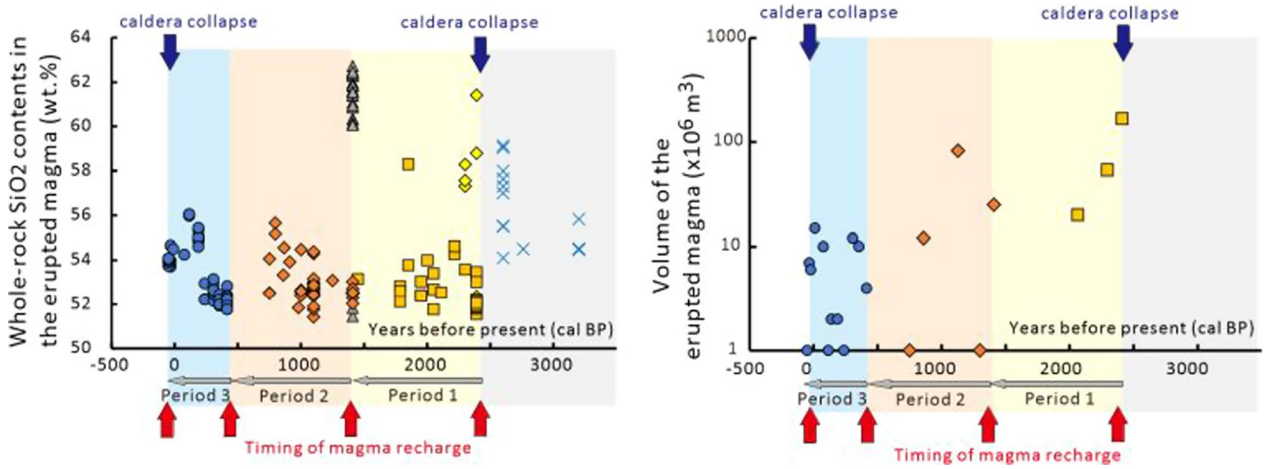

Introduction

Temporal changes in the magma discharge rate, frequency of eruptions and the petrological characteristics of magmas erupted from a volcano may reflect the supply of magma into the plumbing system, compositional evolution in the magma chambers, mixing of compositionally distinct magmas, and extraction of magmas by repeated eruptions and intrusions (Gardner et al. 1995; Matsumoto and Nakagawa 2010; Kuritani et al. 2018). Particularly, injection of hot primitive magmas into a shallow cooler magmatic reservoir may destabilize the magma system and trigger new eruptions with dramatic changes to eruption style (Murphy et al. 1998; Kent et al. 2010). Therefore, investigating temporal changes in the petrological characteristics of erupted magmas can be a powerful tool for monitoring the long-term activity of a volcanic magma system.

Volcanoes with frequent eruptions are favorable targets for investigating the temporal development of a magmatic system. By combining high-precision eruption chronologies with petrological characteristics of the eruptive products, we can reconstruct the evolution of the magma supply system (e.g., Colima; Luhr et al. 2010, Soufriere; Lindsay et al. 2013, Campi Flegrei; Forni et al. 2018, Mt. Usu; Tomiya and Takahashi 1995). However, due to the limited exposure of the erupted materials and lack of high-resolution age data, very few volcanoes can provide eruption sequences with both detailed petrologic data sets and well-constrained chronologies. Miyakejima volcano is an ideal target to study the temporal evolution of a basaltic magmatic system because of frequent eruptions, which vary widely from effusive to sub-Plinian (Tsukui and Suzuki 1998; Geshi and Oikawa 2014). The long-term behavior of Miyakejima is characterized by a cyclic pattern of stratovolcano growth and collapse caldera formation (Niihori et al. 2003; Tsukui et al. 2005). Here, we focus on the change of the magmatic activities of Miyakejima within the last ~2300 years, between two caldera-forming eruptions. Based on our new radiocarbon age constraints and expanded whole-rock geochemical data set for erupted magmas, we reveal that the temporal variations in eruptive activity are controlled by the intermittent injection of primitive magmas into a storage system, which leads to episodic eruption of hybrid magmas that evolved principally by fractional crystallization processes.

Summary of previous studies of Miyakejima

Geology and eruption history

Miyakejima volcano forms a volcanic island named Miyakejima in the northern part of the Izu–Bonin arc (Fig. 1). The island has a circular shape with a diameter of ~8 km and a summit height of ~750 m above sea level. Miyakejima volcano is one of the most active volcanoes in the northern part of the Izu–Bonin arc, with more than 10 eruptions recorded within the last ~300 years. Reflecting the high frequency of eruption, more than 90% of the subaerial island surface is covered by lavas and tephra deposit erupted within the last 12,000 years. Supported by excellent exposure, decades of geological investigations have revealed the stratigraphic relations of the erupted materials of the volcano (Isshiki 1960; Tsukui and Suzuki 1998; Tsukui et al. 2001, 2005).

Reliable historical records cover eruptions younger than the seventeenth century. The preceding eruption history needs to be constructed from the stratigraphic relationship of the ejecta together with new

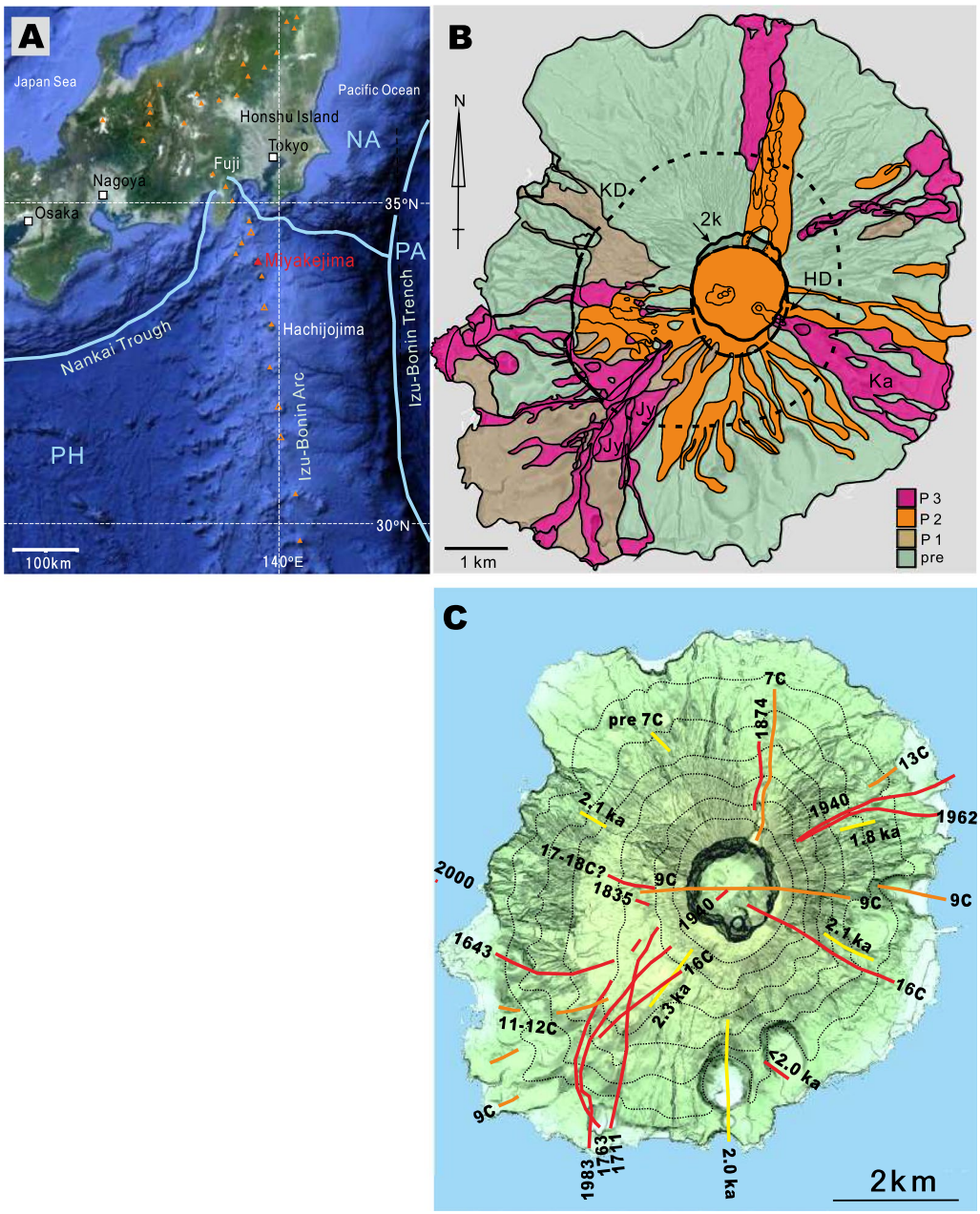

Fig. 1 **A** Location map of Miyakejima volcano. Broad blue lines show the plate boundary. *PH* Philippine Sea Plate, *PA* Pacific Plate, *NA* North American Plate. Orange triangles show the location of active volcanoes. Background image is after Google Earth. **B** Simplified geological map of Miyakejima volcano. Broad black lines show the topographic rim of Kuwanokidaira caldera (KD), Hatchodaira caldera (HD), and the 2000 AD caldera (2k). Dotted line is the buried caldera rim of Kuwanokidaira and Hatchodaira calderas. Pre: edifice of pre-Hatchodaira caldera (older than ~ 2.3 ka). P1: distribution of the deposits of Period 1. P2: the deposits of Period 2 (from seventh to fourteenth century). P3: the deposits of Period 3 (from sixteenth century to present). Distribution of Jinanyama scoria cone and Kamakata lavas are indicated by Jy and Ka, respectively. **C** Distribution of the representative eruption fissures of Period 1 (yellow), Period 2 (orange) and Period 3 (red). Due to the cover of the younger deposits, not all the eruption fissures are identified

radiocarbon age constraints. Tsukui and Suzuki (1998) summarized the stratigraphic relationship of the eruption deposits within the last 7000 years using the identification of key tephra layers that can be traced over the whole island. In particular, fine-grained tephra layers associated with large-scale phreatomagmatic eruptions are useful marker beds because of their relatively wide distribution and recognizable lithofacies. Two

exotic rhyolitic tephra-fall deposits of the AD 838 eruption and the AD 886 eruption of the Kozushima and Niijima volcanoes 30 km to the northwest also cover Miyakejima, and are also identified as valuable chronostratigraphic markers. Based on the pattern of the eruption activities and the whole-rock chemical composition of the erupted magmas, Tsukui and Suzuki (1998) divided the activity of Miyakejima within the last ~7000 years into the stages of Ofunato (older than 7 ka), Tsubota (7–4 ka), Oyama (2.5 ka to AD 1469) and Shinmio (AD 1469 to 1983). Tsukui et al. (2005) summarized the geology and stratigraphy of the volcano based on Isshiki (1960) and Tsukui and Suzuki (1998). Geshi et al. (2019) showed that the Suoana–Kazahaya tephra erupted from the northern slope of the volcano in the seventh century can be traced over the volcano, and therefore, it is also a good time marker.

Magmatic system of Miyakejima

Miyakejima has erupted tholeiitic basaltic to andesitic magmas (Amma-Miyasaka and Nakagawa 1998, 2002, 2003; Kuritani et al. 2003; Niihori et al. 2003; Yokoyama et al. 2003, 2006; Amma-Miyasaka et al. 2005; Saito et al. 2010; Ushioda et al. 2018). The erupted products within the last 2300 years commonly provide evidence for the mixing of two major compositionally distinct magmas, such as linear variation of whole-rock compositions, bimodal distribution of phenocryst chemical compositions, and dissolved, resorbed and reversely zoned phenocryst textures (Amma-Miyasaka and Nakagawa 2003; Kuritani et al. 2003; Niihori et al. 2003; Saito et al. 2010). Based on the temporal change of the compositions of the erupted magmas, Niihori et al. (2003) suggested that periodic injection of the basaltic magma into the shallow andesitic magma chamber causes the mixing and fractional crystallization trends.

Reconstruction of the eruption history

In this study, we examine the stratigraphic relationships of the ejecta of Miyakejima, using observations from new outcrops and results from a comprehensive ^{14}C dating campaign (Fig. 2 and Table 1). The revised stratigraphy is summarized in Fig. 2. We focus on the evolution of the magmatic system between the last two caldera-forming eruptions, which occurred at the eruption occurred after the Hatchodaira eruption (~2.3 ka) and prior to the AD 2000 eruption. This period corresponds to the Oyama stage and Shinmio stage of Tsukui and Suzuki (1998).

The Hatchodaira eruption at ~2.3 ka

The Hatchodaira eruption resulted in the formation of a 2-km-wide collapse caldera (Hatchodaira caldera) at the summit of Miyakejima (Tsukui and Suzuki 1998). The associated products consist of basal scoria fall deposits (Hatchodaira scoria; Tsukui and Suzuki 1998) and overlying fine-grained tephra layers (Hatchodaira ash; Tsukui and Suzuki 1998) associated with a phreatomagmatic pyroclastic density current (PDC). No clear evidence for the time-gap is recognized between the scoria fall deposit and overlying PDC deposit.

Distributions of the scoria fall deposit and partially sintered scoriaceous spatter deposits (Fig. 3A) suggests that the scoria was erupted from a fissure on the southwestern slope of the volcano. The distribution of the overlying PDC deposit (Hatchodaira ash; Fig. 3B) suggests that it was sourced from the summit area. The low abundance of juvenile material and the presence of hydrothermally altered fragments in the ash component of the Hatchodaira ash indicates the eruptive activity of the PDC was driven by phreatomagmatic explosions. The sedimentary structures of Hatchodaira ash, which consist of fine-grained volcanic ash layers with cross bedding and dunes, indicate that it was emplaced by a PDC which flowed down from the summit. The accretionary-lapilli rich deposit contains casts of non-carbonized fragments of plants, suggesting that the deposit was deposited as a wet and relatively low-temperature PDC. However, many juvenile bombs with chilled margins including prismatic joints and glassy rinds are also found in the Hatchodaira ash bed. The ^{14}C ages obtained from a wood piece in the scoria-fall deposit (2280 ± 30 yrBP, which corresponds to 2351–2301, 2248–2158 cal BP) indicates that the Hatchodaira eruption occurred at ~2.2–2.3 ka.

Eruptions between 2.3 ka and the seventh century

The distributions and stratigraphic relations of products from eruptions that occurred between the Hatchodaira eruption and the Suoana–Kazahaya eruption in the seventh century remain uncertain because of their limited exposure due to burial by younger eruptive products. Most of the erupted materials during this period were ejected from, and filled, the interior of the Hatchodaira caldera, which also makes it difficult to understand the eruptive history during this period.

The caldera-filling deposits inside the Hatchodaira caldera are exposed on the wall of the AD 2000 caldera (Fig. 4A). The uppermost 20–30 m of the caldera-filling deposit consists of the Oyama lava erupted in the ninth century. The tephra layer of the Suoana–Kazahaya eruption is exposed below the Oyama lava, at around 650 m asl in the wall of the AD 2000 caldera. Below the Suoana–Kazahaya tephra, >300-m-thick caldera-filling deposits are exposed in the caldera wall. The caldera-filling deposits below the Suoana–Kazahaya tephra are mostly composed of a coherent sequence of alternating lava flows,

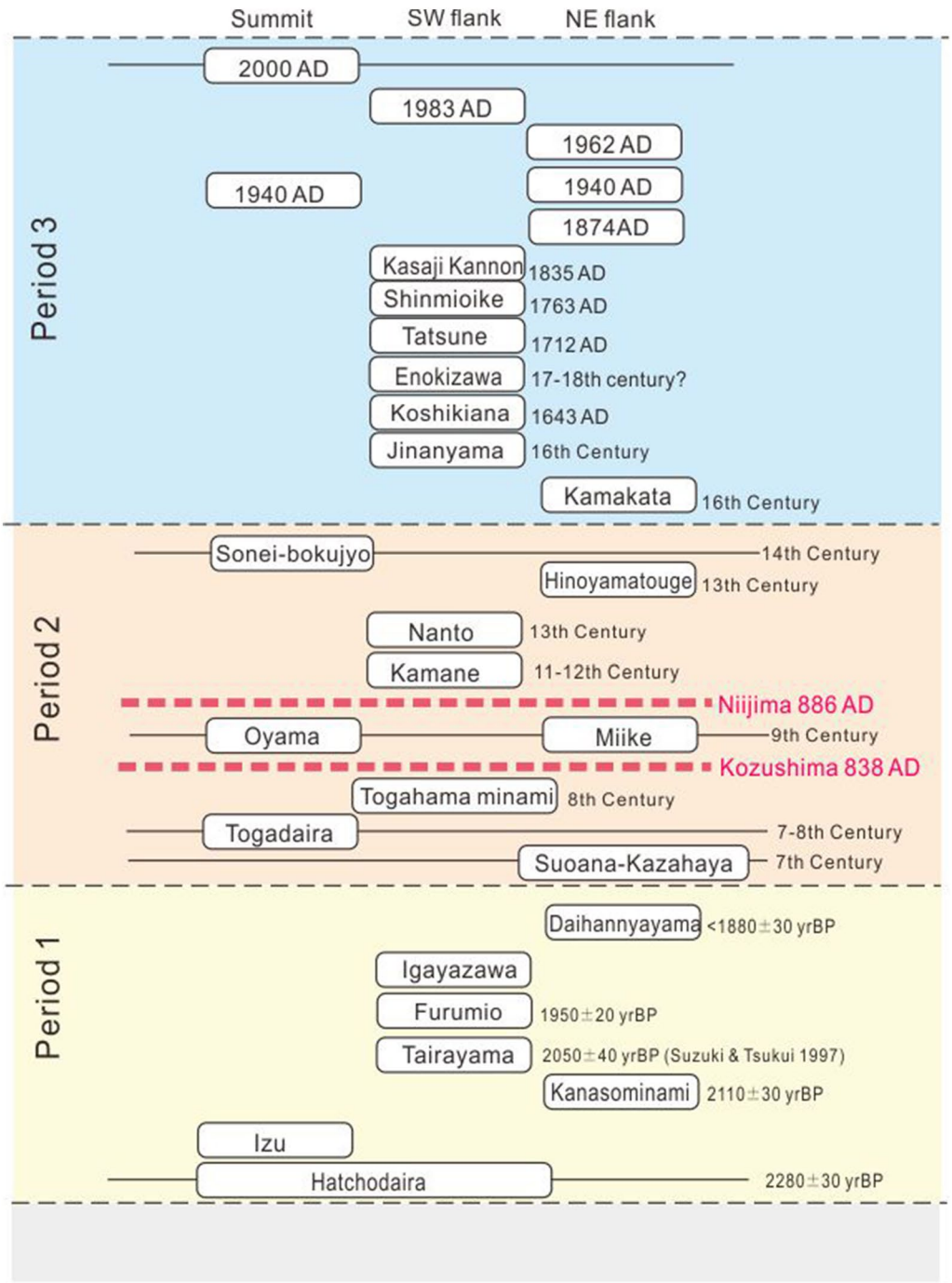

Fig. 2 Schematic stratigraphic relationship of the eruptions during periods 1, 2 and 3. Horizontal solid lines show the key tephra beds which cover the entire island. Note that there are several eruption products that have unfixed (approximated) stratigraphic positions particularly during Period 1 and 2

except for the uppermost few tens of meters. The stratigraphy of the caldera-filling deposits (Fig. 4) indicates that the Hatchodaira caldera was rapidly filled within about 1000 years of its formation with the lavas erupted inside the caldera.

The post-Hatchodaira deposits outside of the caldera can be observed in several outcrops on the slopes of the volcano (Figs. 4B and 5), though most of the products of this period are covered by younger deposits. Figure 6A shows the distribution of the scoria cone deposits

Table 1 Age of eruptions stratigraphycally younger than Suoana-Kazahaya

Eruption	Eruption site	Age			Magma volume (DRE)	Note
		AD/BC	^{14}C age	Calibrated age (yr BP) (98%)	$\times 10^6$ m^3	
Period 3						
2000 AD	Summit	2000 AD			<1[d]	Age confirmed by historical records
1983 AD	SW flank	1983 AD			7[c]	Age confirmed by historical records
1962 AD	NE flank	1962 AD			6[c]	Age confirmed by historical records
1940 AD	NE flank	1940 AD			15[c]	Age confirmed by historical records
Meiji	N flank	1874 AD			16[e]	Age confirmed by historical records
Kasaji-kannon	W upper flank	1835 AD			<1[c]	Age confirmed by historical records
Enokizawa	W upper flank	Not confirmed by record	120 ± 20 yrBP[g] 70 ± 20 yrBP[g]	256–222 cal BP 138–31 cal BP	2[c]	
Shinmio-ike	SW flank	1763 AD			5[g]	
Tatsune	SW flank	1712 AD			1[c]	
Koshikiana	W flank	1643 AD			12[c]	Age confirmed by historical records
Jinanyama	SW middle flank	1595 AD?	315 ± 20 yrBP[g]	460–347, 337–306 cal BP	20[g]	
Kamakata	E flank	1535 AD?	340 ± 20 yrBP[g] 380 ± 20 yrBP[g] 390 ± 20 yrBP[g]	477–312 cal BP 509–428, 374–367, 359–328 cal BP	25[g]	Lavas of Benkene-misaki and Kamakata of Tsukui and Suzuki (1998)
Period 2						
Sonei-bokujyo	Summit	14th century			4[c]	
Hinoyamatouge	E flank	13th century?	690 ± 20 yrBP[g] 700 ± 20 yrBP[(6)]	681–644, 587–565 cal BP 685–649, 583–567 cal BP	<1[c]	
Nanto	SW middle flank	13th century	750 ± 20 yrBP[g]	725–667 cal BP	1[c]	
Kamane	SW flank	11–12 century	860 ± 20 yrBP[g]	900–870, 800–720 cal BP	12[c]	
(Mukaiyama pumice of Niijima volcano)		886 AD				Age confirmed by historical records
Oyama	Summit, E-flank	9th century	1240 ± 20 yrBP[g]	1263–1121, 1113–1083 cal BP	82[c]	
(Tenjosan pumice of Kozushima volcano)		838 AD				Age confirmed by historical records
Togahama minami lava	SW flank	9th century			<1[c]	
Togadaira	Summit?					
Suoana-Kazahaya	N flank	7th century	1360 ± 20 yrBP[e] 1410 ± 30 yrBP[e]	1306–1270 cal BP 1359–1285 cal BP	25[f]	
Period 1						
Furumio ash	S flank		1950 ± 20 yrBP[g]	1935–1824 cal BP		
Tairayama scoria	NW flank		2050 ± 40 yrBP[ab]	2119–2011 cal BP	20[c]	
Kanaso south	E flank		2110 ± 20 yrBP[g]	2143–2138, 2126–2000 cal BP		
Izu scoria	Summit				50[c]	Above the Hatchodaira scoria
Hatchodaira scoria	SW flank		2280 ± 30 yrBP[g]	2351–2301, 2248–2158 cal BP	170[c]	

[a] 14C data obtained from a carbonized material beneath the layer

[b] Suzuki and Tsukui (1997)

[c] Tsukui and Suzuki (1998)

[d] Geshi and Oikawa (2008)

[e] Japan Meteorological Agency (2013)

[f] Geshi et al. (2019)

[g] This study

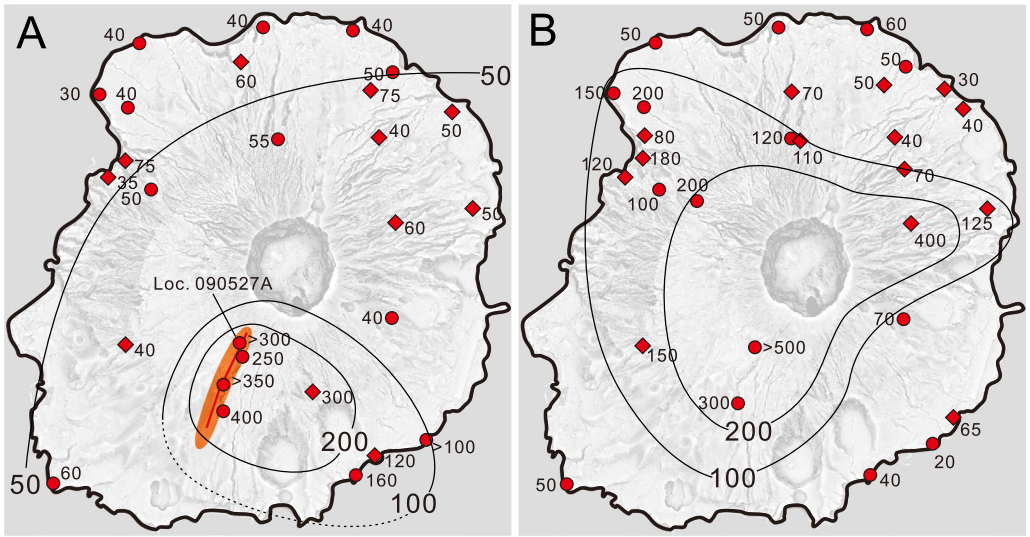

Fig. 3 Distribution of the Hatchodaira scoria fall deposit (**A**) and the Hatchodaira ash layer (**B**). Orange area in **A** shows the approximate distribution of the welded spatter. Circle symbols show the field measurement by this study, and diamond symbols show the data shown by Tsukui and Suzuki (1998)

and lava flows erupted during Period 1. Except for in the vicinity of the lateral eruption fissures, the thickness of the Period 1 ejecta above the Hatchodaira ash deposit is 3–5 m on the middle slope and 1–2 m near the coast (Fig. 5).

Eruptions between the seventh and ninth century

The Suoana–Kazahaya eruption (Geshi et al. 2019) was a relatively large fissure eruption in the last ~2300 years that occurred from the upper part of the northern slope of the island (Fig. 6B). This eruption involved extensive lava fountaining that produced a thick tephra sheet at the beginning of the eruption, i.e., no lava flow was produced. The tephra from the Suoana–Kazahaya eruption covers the entire island, but is particularly thick in the northeastern part of the island. The field investigations revealed that the Togadaira scoria and Mitoribata scoria described by Tsukui and Suzuki (1998) are a part of the tephra of the Suoana–Kazahaya eruption. The ^{14}C ages obtained from the tephra deposit of the Suoana–Kazahaya eruption (1360 ± 20 yr BP, which corresponds 644–680 cal AD) show that the eruption occurred in the seventh century.

The Togadaira ash is a fine-grained volcanic ash layer composed mainly of non-juvenile materials. The Togadaira ash overlies a thin paleosol above the tephra of Suoana–Kazahaya eruption. Although no ^{14}C age was obtained from the Togadaira ash, the presence of many casts of tree trunks in the secondary deposit of the Togadaira ash deposited inside the crater of the Suoana–Kazahaya eruption suggests that there was a time lag between the Suoana–Kazahaya eruption and the eruption of Togadaira ash, when a shrubby forest was formed in the crater. Judging from the typical recovery time scale of forest in the eruption-devastated area in Miyakejima, the timescale between the Suoana–Kazahaya and Togadaira eruptions can be ~10 years or more. Togahama–minami lava is a product of a lateral eruption that is present locally on the southwestern coast of the volcano (Figs. 2D and 6B). The Togahama–minami lava is covered by the Kozushima Tenjosan AD 838 tephra and overlies the Togadaira ash.

The Oyama eruption was fed by an E–W aligned fissure system that crossed the summit of the volcano (Fig. 6B). The eruption produced lava flows (Oyama lava), scoria fall (Oyama scoria) and phreatomagmatic explosion breccia (Miike explosion breccia) with associated PDC and ash fall deposits (Fig. 7). The ejecta of the Oyama eruption overlies the rhyolitic ash fall deposit of the Kozushima Tenjosan AD 838 eruption (Fig. 4C). A new ^{14}C age obtained by this work (1240 ± 20 BP, which corresponds to 1263–1121, 1113–1083 cal BP, Table 1) is consistent with stratigraphic relationships.

Eruptions between the eleventh and sixteenth century

At least four tephra layers (Kamane, Hinoyamatouge, Nanto and Sonei–bokujyo; Tsukui and Suzuki 1998) are recognized between the Niijima Mukaiyama tephra erupted in AD 886 and the Kamakata tephra erupted in the sixteenth century (Fig. 2). The distribution of the ejecta of these eruptions shows that tephra of

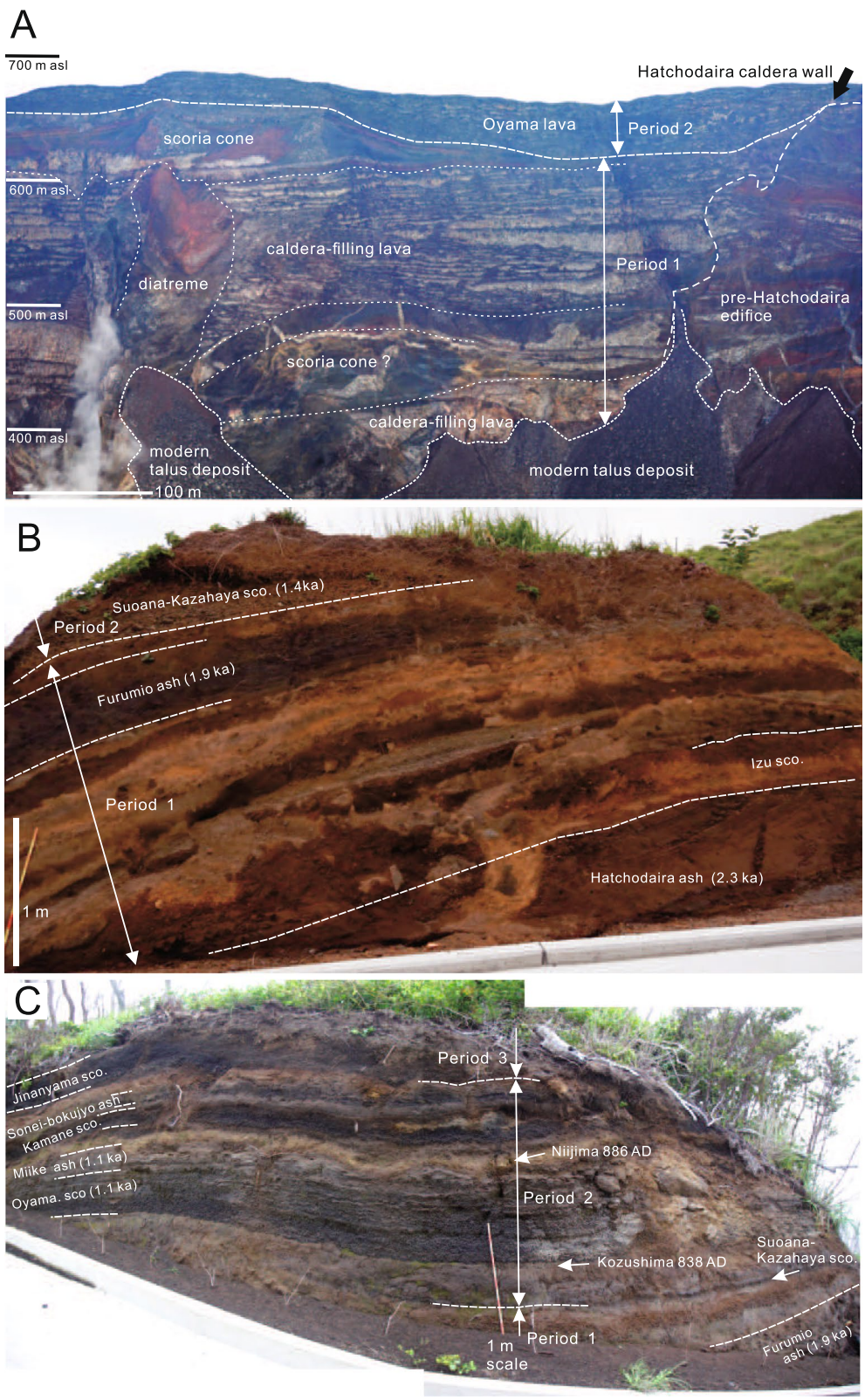

Fig. 4 **A** Caldera-filling deposits inside the Hatchodaira caldera exposed on the southwestern wall of the 2000 AD caldera. **B** Fall-out deposits of Period 1 overlying on the Hatchodaira ash. Location E2 of Fig. 5. **C** Fall-out deposit of Period 2 and 3 Location D of Fig. 5

Hinoyamatouge, Nanto and Kamane erupted from fissures on the flank of Miyakejima (Fig. 6C). The Sonei–bokujyo tephra was erupted from the summit area. The obtained ^{14}C ages indicate that the Hinoyamatouge eruption and Nanto eruptions occurred in the thirteenth century, and the Kamane eruption occurred in the eleventh–twelfth century (Table 1).

Several small scoria beds are also found between the Niijima AD 886 tephra and Sonei–bokujyo tephra, but their stratigraphic relationships and ages have not yet been identified due to their limited exposure (Fig. 5). These may be ejecta from unknown eruptions that were not identified in this study.

Eruptions in the sixteenth century

We found that two eruptions occurred on the southwestern and eastern flanks of the island, likely around the sixteenth century (Figs. 6D and 8). A layer of the eruption products was found around an eruption fissure trending east from the summit area on the eastern flank of the island (Fig. 6D). The eruption fissure fed the Benkenemisaki and Kamakata lavas (Tsukui and Suzuki 1998), and associated scoria-fall deposit mainly in the eastern part of the island. Hereafter, we call this eruption the Kamakata eruption, after the name of the lava flow. This scoria-fall deposit overlies a paleosol above the Sonei–bokujyo ash of the fourteenth century, and is covered by the tephra of the AD 1712 and 1763 eruptions. This stratigraphic relationship and the ^{14}C age obtained from the scoria fall deposit of the Kamakata eruption suggest that the eruption also occurred in the sixteenth century. The total volume of the erupted magma of the Kamakata eruption is estimated to be $\sim 2.5 \times 10^{-2}$ km^3 in DRE.

Another scoria-fall deposit is found around the Jinanyama scoria cone on the southwestern slope of the island (Fig. 6D). Alignment of the scoria cone and craters of Jinanyama shows that the eruption was fed by an eruption fissure trending NE–SW. Scoria-fall deposit from this eruption overlies the paleosol above the Sonei–bokujyo ash, and is covered by the tephra of the AD 1712 and AD 1763 eruptions. This stratigraphic relationship and

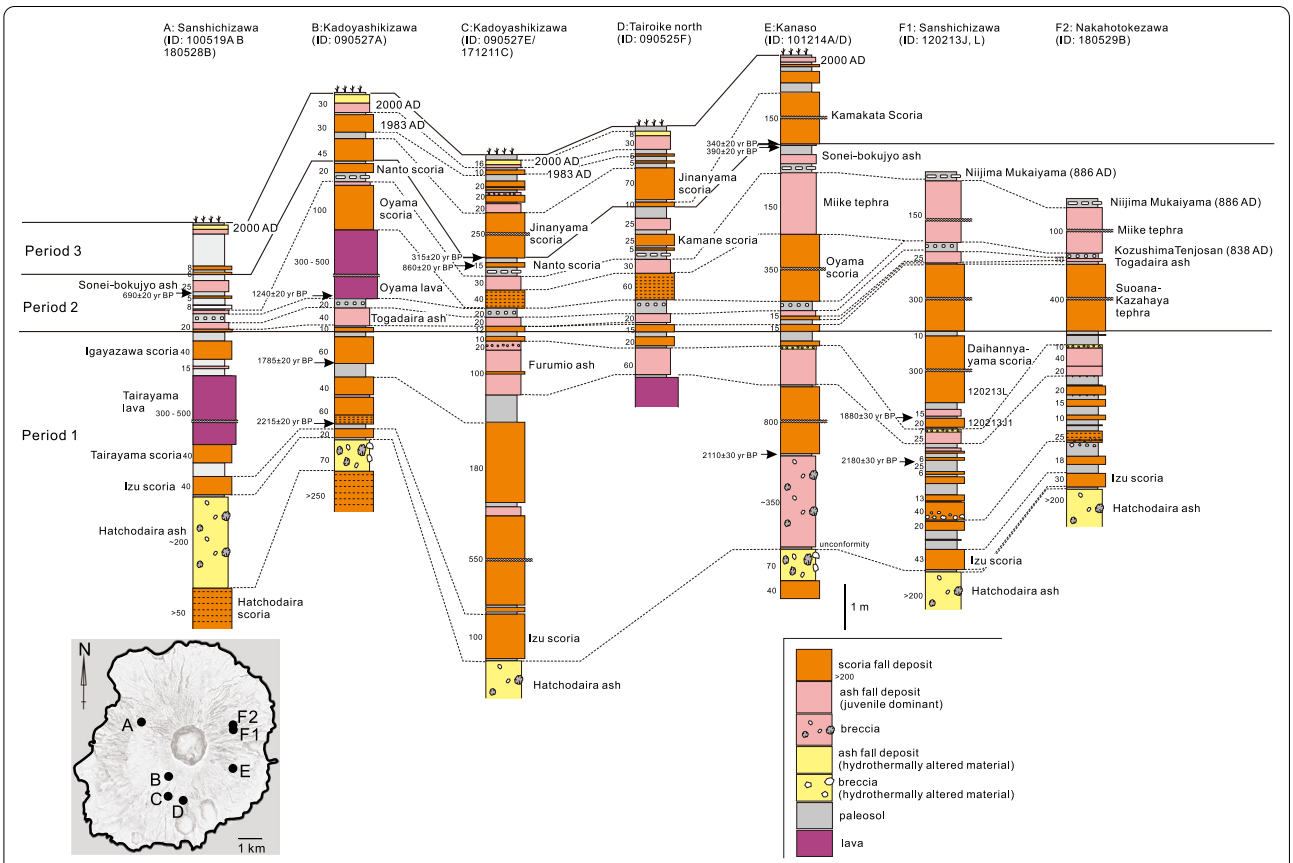

Fig. 5 Stratigraphy of representative outcrops. **A** Tairayama on the northwestern slope, **B** Kadoyashikizawa on the southwestern slope, **C** Tatsunezawa on the southwestern slope, **D** Tairoike north on the southern slope, **E** Kanaso–minami on the eastern slope, F1: Sanshichizawa on the eastern slope, F2: Nakahotokezawa on the eastern slope. The unit of the thickness is in cm

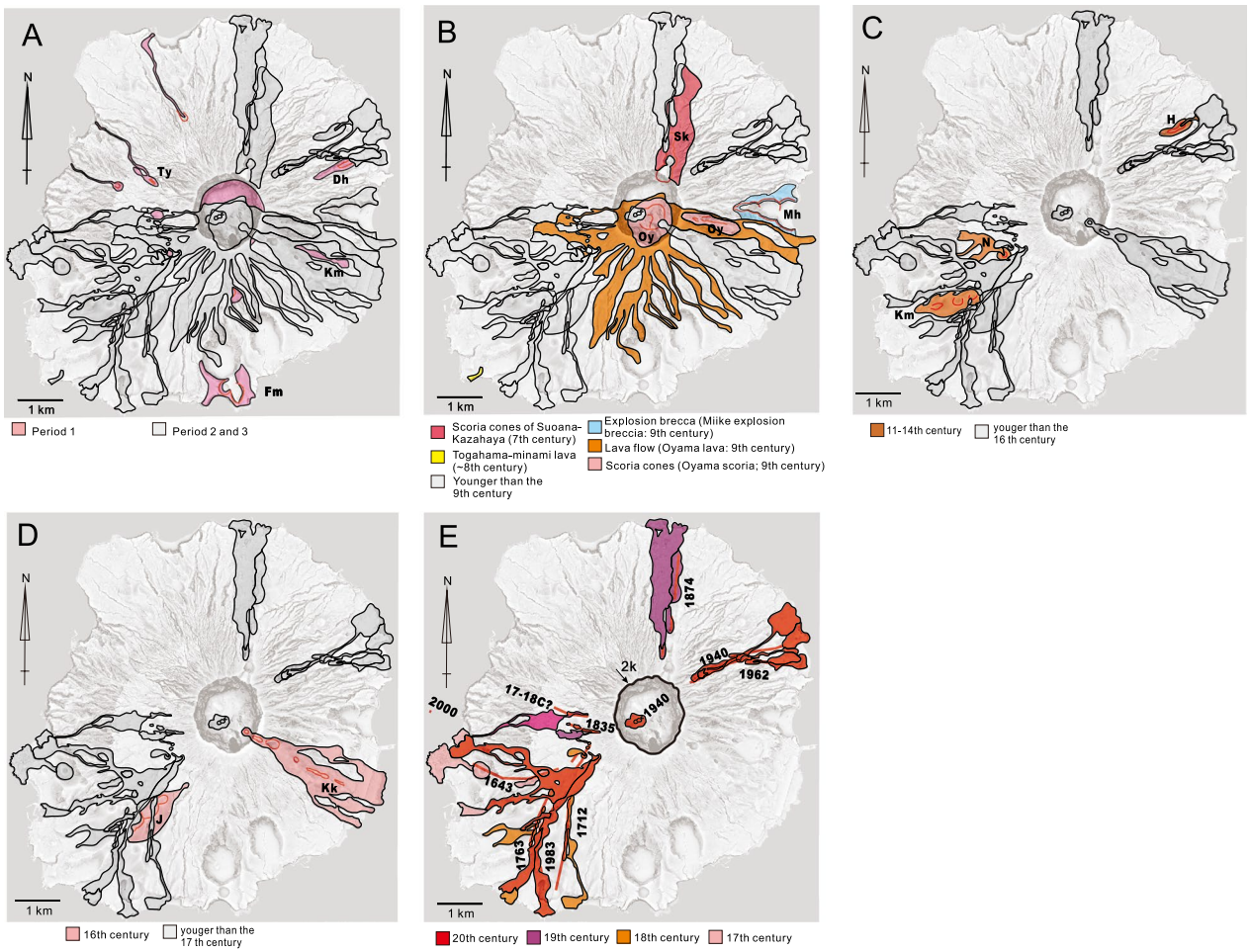

Fig. 6 Distributions of the eruption products (lava flows and scoria cones). The hill-shade map uses the topography after the 2000 AD eruption. **A** Period 1 products between 2.3 ka and seventh century. Representative lateral eruption fissures are shown. Kanasominami (Km), Tairayama (Ty), Furumio (Fm), Daihannyayama (Dh). **B** the eruption products between seventh and ninth century (Period 2). Suoana–Kazahaya (Sk), Oyama (Oy), Miike (Mh). **C** The eruption products between the ninth and fourteenth centuries. Kamane (Km), Nanto (N) and Hinoyamatouge (H) in Period 2. **D** The eruptions of Jinanyama (J) and Kamakata (Kk) possibly in the sixteenth century (beginning of Period 3). **E** The eruptions between the seventeenth and twentieth centuries (Period 3) with their eruption age. "2k" indicate the caldera rim formed by the 2000 AD eruption

the ^{14}C age obtained from charcoal in the scoria-fall deposit (320 ± 20 BP, which corresponds to 1490–1603, 1613–1644 cal AD) suggest that the eruption occurred in the sixteenth century. The total volume of the erupted magma is estimated to be $\sim 2 \times 10^{-2}$ km^3 in DRE. Though the obtained ^{14}C ages for each ejecta were overlapping (Table 1), the stratigraphic relationship of their tephra beds indicates that the Jinanyama eruption is younger than the Kamakata eruption. These two eruptions may correspond to the events in AD 1535 and AD 1595 that are recorded in ancient documents.

Eruptions between the seventeenth and twentieth century

The observed vent locations and distributions of the products of the youngest nine eruptions in AD 1643, 1712, 1763, 1835, 1874, 1940, 1962, 1983 and 2000 (Fig. 6E) are consistent with the historical records summarized by Tsukui and Suzuki (1998) and Tsukui et al. (2005). Among them, the eruptions of AD 1874, 1940, 1962, 1983 and 2000 have been documented by many scientific reports (Tsukui et al. 2005 and references therein). Based on the historical record, the Ako–Imasaki lava fed from the Koshikiana scoria cone is identified as the product of the Koshikiana eruption in AD 1643. The lava flow of Kasaji–kannon in the western middle slope is identified as the product of the AD 1835 eruption.

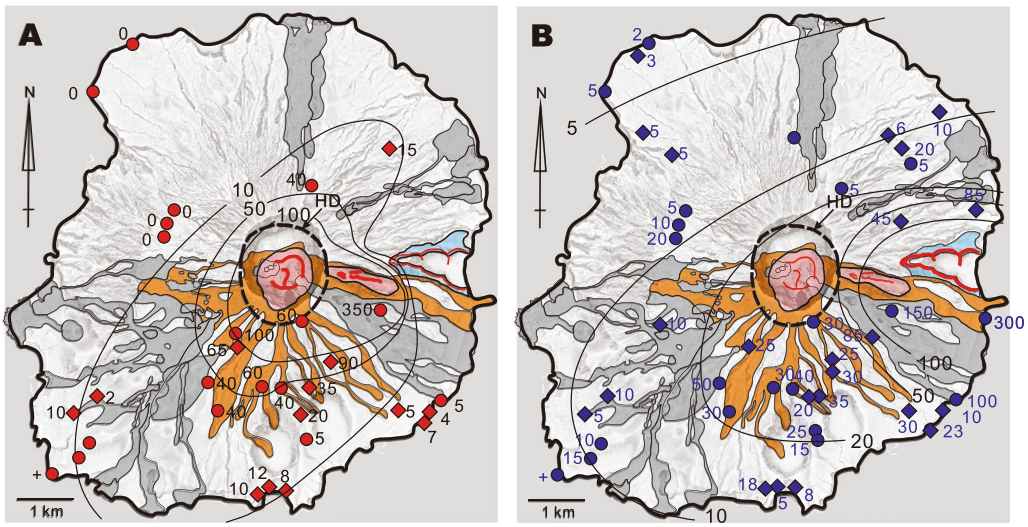

Fig. 7 Distributions of the Oyama scoria fall deposit (**A**) and Miike explosion breccia and associated PDC and ash-fall deposit (**B**) produced during the Oyama eruption. Orange area shows the distribution of the Oyama lava. Gray areas show the distribution of the deposits younger than the Oyama eruption. Circle symbols show the thickness data of these deposits by our field survey, and diamond symbols show the data after Tsukui and Suzuki (1998)

Based on the results of our field surveys, the following changes were made to the eruption history from previous studies, such as Tsukui and Suzuki (1998) and Tsukui et al (2005) (see Appendix Fig. 12). (1) The ejecta of "the AD 1811 eruption", which is an eruption from the summit area described in the historical records (Tsukui and Suzuki 1998), could not be identified by our field survey. (2) Though the Enokizawa lava that outcrops in the western slope has been considered to be the product of the AD 1469 eruption (Tsukui and Suzuki 1998), we found a scoria fall deposit possibly associated with the Enokizawa lava and obtained two ^{14}C ages (120 ± 20 BP and 70 ± 20 BP, which correspond to 1694–1728 and 1812–1919 cal AD, respectively). The scoria fall deposit overlies the Sonei–bokujyo ash and, is covered by the product of the 1835 eruption. (3) Based on the topographical analysis using a 5-m-grid digital elevation map and the geological survey, we identified two eruption fissures on the southern slope of the Jinanyama scoria cone which was formed in the sixteenth century. As interpreted by Tsukui and Suzuki (1998), the eastern eruption fissure is thought to have been formed by the AD 1712 eruption. The western eruption fissure is thought to have been formed by the AD 1763 eruption, which formed Shinmioike maar.

Whole-rock geochemistry

We examine the whole-rock compositions of the erupted magmas within the last ~2300 years based on the reconstructed distribution and stratigraphy of the ejecta. Whole-rock compositions of eruptive products are shown in Additional file 1: Fig. S1 and Additional file 2: Table S1. Analytical method is shown in Appendix.

Most of eruptive products within the last ~2300 years are basaltic andesites, with subsidiary basaltic and andesitic volcanic material (Fig. 9). Several andesitic magmas with whole-rock SiO_2 contents greater than 58 wt% were erupted (e.g., juvenile bombs in the Hatchodaira ash, and the aphyric andesite erupted during the Suoana–Kazahaya eruption). Based on the relationship between eruption age and magma composition, we have divided the eruption history of Miyakejima within the last ~2300 years, from the formation of the Hatchodaira caldera, into three period as follows: Period 1 occurs between the Hatchodaira eruption at ~2.3 ka and the seventh century Suoana–Kazahaya eruption. Period 2 started with the eruption of basaltic magmas in the Suoana–Kazahaya eruption in the seventh century and continued to the fourteenth century Sonei–bokujo eruption. Period 3 started with the Kamakata eruption in the sixteenth century and continued to the AD 2000 eruption (Fig. 10).

The start of Period 1 is marked by the eruption of a Hatchodaira scoria, which has a basaltic composition with 51.5–53.5 wt% whole-rock SiO_2, from the lateral fissure in the southwestern slope. The eruption of the Hatchodaira scoria was followed by the eruption of andesitic magmas with whole-rock SiO_2 ranging from 58 to 62 wt% from the summit. A vigorous phreatomagmatic eruption of the andesite magma produced Hatchodaira ash. The Izu scoria, which erupted from the summit just

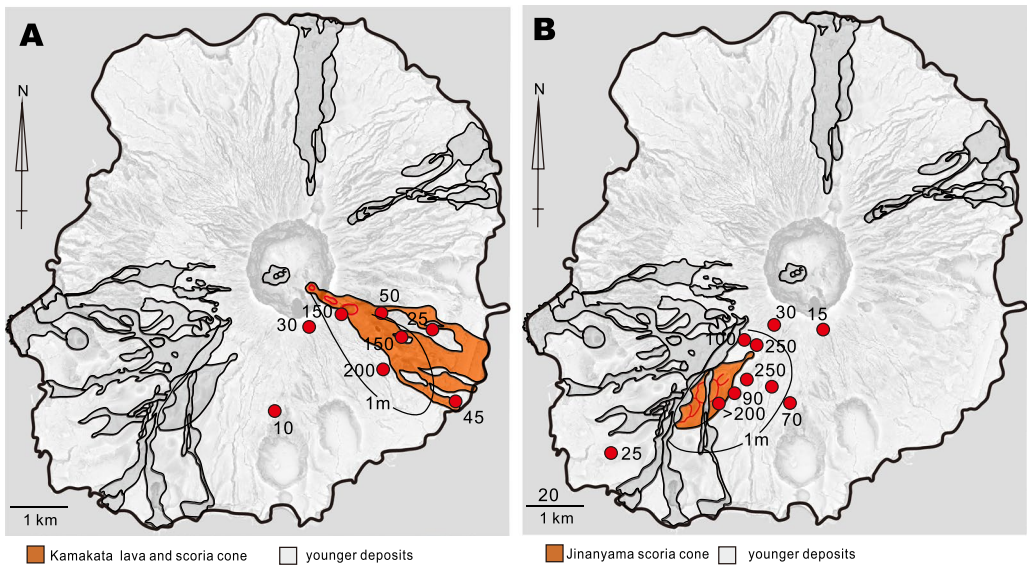

Fig. 8 Distributions of the deposits of Kamakata eruption (**A**) and Jinanyama eruption (**B**), which occurred in the sixteenth century. Red circles show the measurement points of thickness of the scoria fall deposit of each eruption. Gray areas show the distribution of the deposits younger than the eruptions

after the formation of the Hatchodaira caldera, also has a high whole-rock SiO_2 content ranging between 57 and 59 wt%, which is similar to those of the bombs in the Hatchodaira ash erupted from the summit. The chemical composition of the lava flows filling the caldera, which erupted from the "summit", is unknown, because direct sample collection has not been realized so far.

The products from the lateral fissure eruptions during Period 1 are characterized by basaltic andesite compositions with whole-rock SiO_2 ranging from 51.8 to 54.6 wt%, clearly lower than those of the products from the summit area (Hatchodaira ash and Izu scoria; Fig. 10). Igayazawa scoria, which is thought to have erupted from a fissure on the northwestern flank of the mountain (Tsukui and Suzuki 1998), has exceptionally high whole-rock SiO_2 reaching 58 wt% (Fig. 10).

The start of Period 2 is marked by the Suoana–Kazahaya eruption, which produced basaltic magmas with whole-rock $SiO_2 \sim 51.5$–53.0 wt% at its later stage. There was a slight upward shift in the range of the whole-rock SiO_2 contents of the erupted magmas during Period 2 which increased to 52.5–55.7 wt% at Hinoyamatouge and Sonei–bokujo eruptions at ~0.7 ka. The whole-rock FeO*/MgO ratio and whole-rock concentrations of K_2O, P_2O_5, Cu, Zn, Sr, Zr and Ba also increase through Period 2 (Fig. 10).

Period 3 is also characterized by the broadening of the compositional contrast between the evolved andesitic end-member and the coevally erupted mafic parental magmas. The start of Period 3 is marked by the eruption of basaltic magmas from three eruptions in the sixteenth and seventeenth centuries (Kamakata, Jinanyama, and the AD 1643 eruptions), which erupted basaltic magmas with whole-rock SiO_2 from 51.8 to 53.1 wt%. The eruptions in the eighteenth to twentieth centuries ejected basaltic andesitic products with whole-rock SiO_2 ranging from 53.7 to 56.0 wt%, as well as basaltic magmas with whole-rock SiO_2 ranging from 51.5 to 53.0 wt%. Whole-rock FeO*/MgO ratio and whole-rock concentrations of K_2O, P_2O_5, Cu, Zn, Sr, Zr and Ba also increase from the beginning of Period 3 to the AD 1874 eruption. Whole-rock MgO, V, Cr, Cu decrease in this period. After the AD 1940 eruption, these compositional trends appear to be reversed toward the AD 2000 eruption (Fig. 10).

Magma eruption rate

The erupted volume of magmas and the magma production rate are largest during Period 1, and decrease from Period 1 to Period 3 (Table1, Fig. 11). Period 1, from ~2.3 ka to the seventh century, corresponds to the period when the Hatchodaira caldera was filled by post-caldera eruptions from the caldera floor. The volume of the lavas filling the Hatchodaira caldera is estimated to be 0.4 km^3 in DRE. This estimation is supported by the assumption that the volume of the Hatchodaira caldera was the same as that of the AD 2000 caldera (0.6 km^3 Geshi et al. 2002) and that the apparent volume of the pile of lavas inside the caldera is 1.5 times greater than the DRE volume of magma, based on the observation that half of the deposit consists of dense lava, and the other half consists

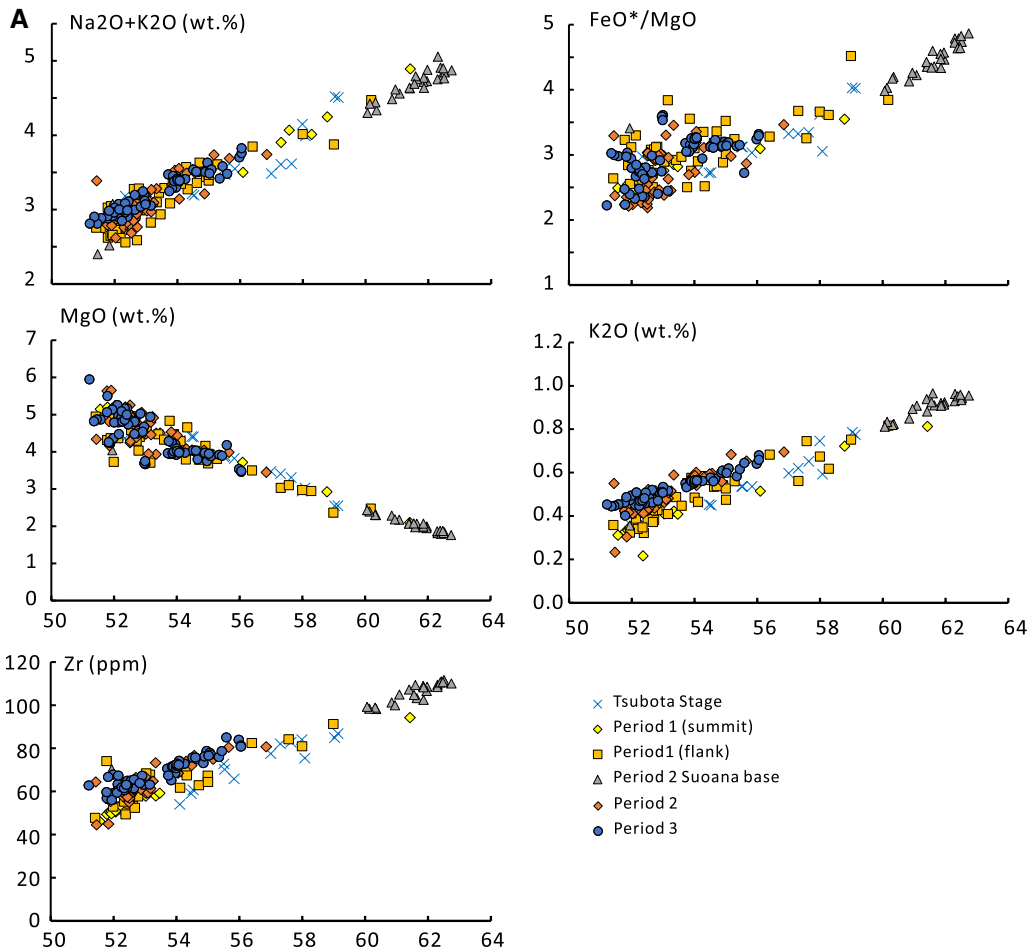

Fig. 9 Whole-rock $Na_2O + K_2O$, MgO, K_2O and Zr contents, and the FeO*/MgO ratio of the magmas within the last 3500 years including Period 1–3 plotted against their SiO_2 contents in weight percent. All plotted data are normalized as total 100%

of scoriaceous clinker. Meanwhile, many lateral fissure eruptions outside the Hatchodaira caldera during Period 1 produced ~0.1 km^3 of magma during Period 1 (Tsukui and Suzuki 1998). Considering the possibility that there may be unrecognized Period 1 ejecta covered by younger deposit, the Period 1 ejecta volume may be slightly larger than this estimate. Therefore, the total volume of the erupted magma during Period 1 is estimated as 0.5 km^3 or more. Among them, approximately 80% of magmas were erupted and deposited inside the Hatchodaira caldera.

Approximately 0.13 km^3 of magmas were erupted during Period 2, from the seventh century to the fourteenth century. Two large eruptions (Suoana–Kazahaya eruption and Oyama eruption) at the early stage of the period produced ~85% of the total volume of the erupted magmas during Period 2.

The total volume of erupted magmas during Period 3 from the sixteenth to twentieth century, is estimated as 0.11 km^3. More than half of the total volume of magmas was erupted by the first three eruptions (Kamakata, Jinanyama, and Koshikiana) within the first ~100 years of the period.

The eruption rate of magma during Period 1 is estimated as ~0.5 km^3 per 1000 years, as the duration of Period 1 is ~1000 years from 2.3 ka to the seventh century. The eruption rate of magma during Period 2, from the seventh century to the fourteenth century, is estimated as ~0.2 km^3 per 1000 years. The magma eruption rate during Period 3, from the sixteenth to twentieth century, is also estimated as ~0.2 km^3 per 1000 years.

Discussion

Explosive large eruptions fed by magma recharge

Cyclic variability of whole-rock compositions in the erupted magmas from more primitive to more evolved during Period 2 and 3, as shown in Fig. 10, implies the

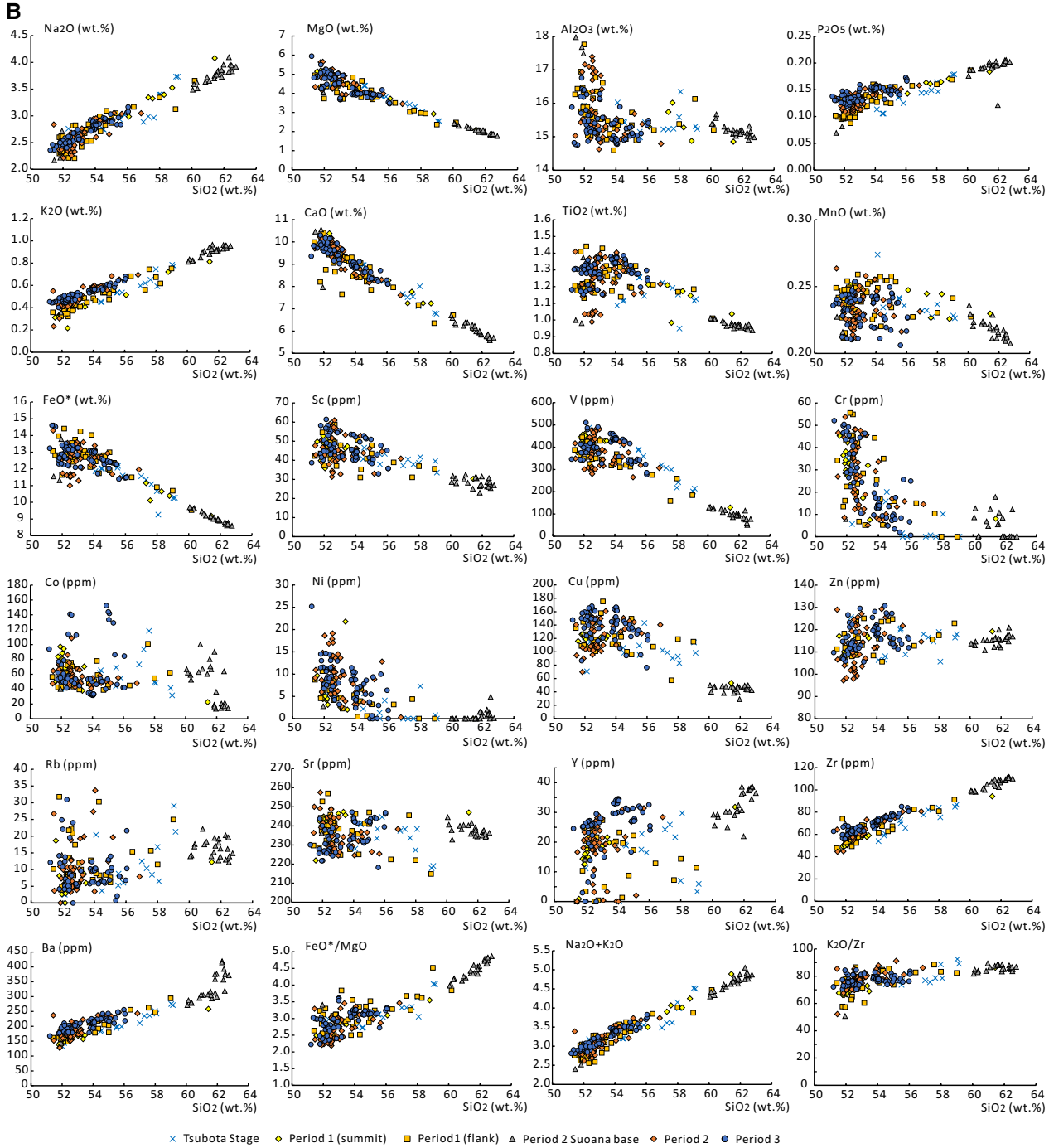

Fig. 9 continued

(See figure on next page.)

Fig. 10 Temporal change of the whole-rock compositions of the erupted magmas in Periods 1, 2 and 3. The vertical line shows the timing of the 1874AD eruption. All plotted data are normalized as total 100%. Only aphyric ejecta of the Suoana–Kazahaya eruption are plotted to eliminate the effect of xenocryst contamination. The eruption ages younger than the seventeenth century are based on historical records. The eruption ages older than the sixteenth century are given as calibrated ages using the IntCal 20 program

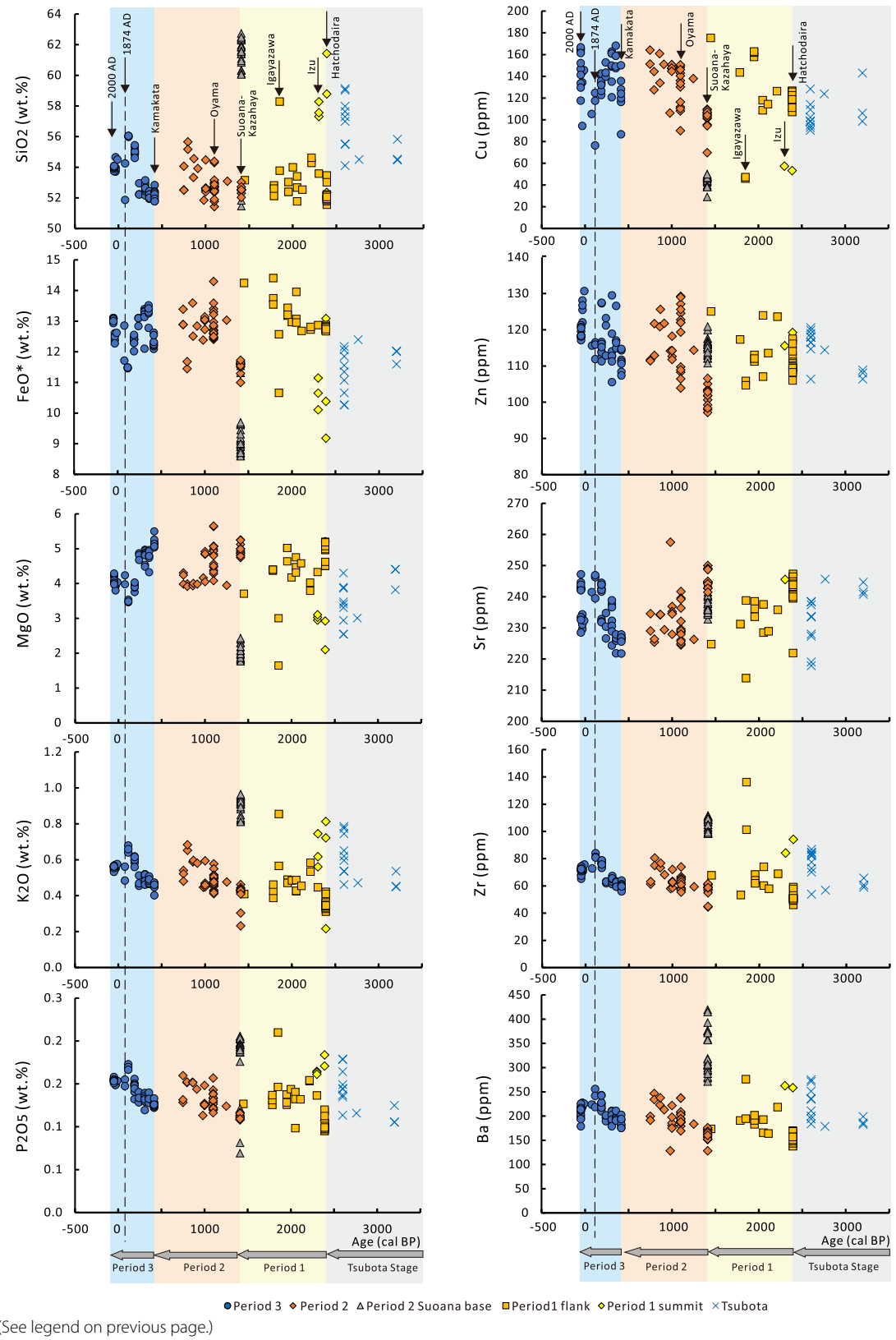

Fig. 10 (See legend on previous page.)

major recharge of mafic magma at the beginning of each period and subsequent fractional crystallization as pointed by Niihori et al. (2003). The basaltic ejecta (Hatchodaira scoria) from lateral eruption fissure at the beginning of the Hatchodaira eruption also indicates the recharge of basaltic magma at the beginning of Period 1, though the magma composition trends during Period 1 are more complicated and not yet well-defined.

The recharge of basaltic magma may cause the eruption with greater volumes of magma at the early part of each period than the following eruptions (Fig. 11). The eruption volumes of these eruptions are much larger than the average volume (0.95×10^{-2} km^3) of magma erupted during the last four lateral fissure eruptions (AD 1874, 1940, 1962 and 1983) which are well confirmed their eruption volumes. The magmatic volume of the Hatchodaira scoria erupted at the beginning of Period 1 is estimated as 1.7×10^{-1} km^3 (Tsukui and Suzuki 1998), which is the largest eruption throughout from Period 1 to Period 3. The Oyama eruption at the beginning of Period 2 produced a total 8.2×10^{-2} km^3 of basaltic magma (Tsukui and Suzuki 1998), which is the largest eruption during Period 2. The Kamakata eruption and the Jinanyama eruption in the early stage of Period 3, produced 2.5 and 2.0×10^{-2} km^3 of basaltic magma, respectively (Table 1).

The recharge of volatile-rich mafic magmas also caused the explosive eruptions at the beginning of each period. The Hatchodaira eruption at the beginning of Period 1 erupted all basaltic magmas as scoria fall-out deposit (Hatchodaira scoria). More than 70% of the ejected magma (3×10^{-2} km^3) of the Oyama eruption was released as scoria, excluding the fine-grained tephra from the phreatomagmatic explosions in the coastal area (Tsukui and Suzuki 1998). The Kamakata and Jinanyama eruptions, which occurred in the early stage of Period 3 were also characterized by a higher ratio of scoria to total erupted materials compared with later eruptions. These explosive activities at the beginning of each period are contrasting with the effusive-dominant activities found in the middle-late stage of each Period.

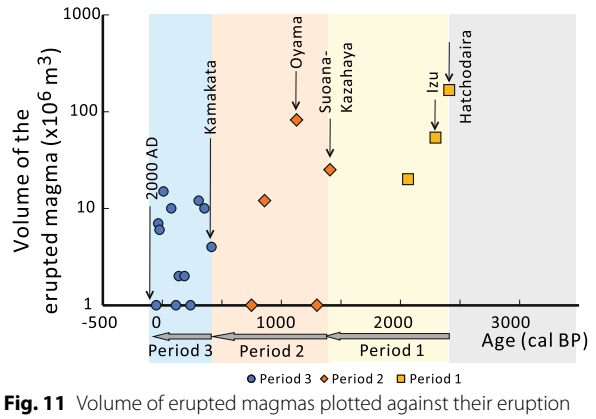

Fig. 11 Volume of erupted magmas plotted against their eruption age. Types of symbols indicate the magmatic periods defined in the text. Note that the volume of the lavas filling the Hatchodaira caldera during Period 1 (~6×10^{-1} km^3) is not shown in this diagram

Explosive eruption hazards

The petrological features of the erupted magmas at Miyakejima discussed above underline two main explosive eruption scenarios at this active volcano. Primarily, recharge of primitive basaltic magmas into the shallow system can cause the explosive eruption of voluminous basaltic magmas. This occurred at the beginning of Period 1 (Hatchodaira scoria eruption), Period 2 (Oyama eruption), and Period 3 (Kamakata and Jinanyama eruptions). Eruptions can be explosive when volatile-rich mafic magmas are injected from a deep-seated source, as reported in many basaltic volcanic systems, such as Mt. Etna (Kamenetsky et al. 2007; Ferlito et al. 2012) and Stromboli (Métrich et al. 2010).

The second potential source for an explosive eruption is the rupturing of an isolated magma body undergoing crystal fractionation. Andesitic magmas with higher SiO_2 and volatile element contents due to fractional crystallization also have the potential to contribute to explosive events, such as the one that occurred during the Suoana–Kazahaya eruption in the seventh century, which started with intense fire-fountaining of evolved andesitic magma. The similarity between the compositions of the andesitic magmas of the Tsubota stage and the Suoana–Kazahaya eruption (Fig. 9) may indicate that the latter were remnant magmas of the Tsubota stage which were stored in an isolated shallow magma chamber for at least 1000 years. Explosive eruption of evolved magma from lateral fissures is also known in other basaltic volcanoes in the Izu islands (e.g., a sub-Plinian eruption from the B fissure of the 1986 Izu–Oshima eruption; Fujii et al. 1988; Endo et al. 1988; Sumner 1998). The danger of sudden eruptions from covert silicic magma bodies within dominantly basaltic volcanoes has also been noted for several volcanoes, such as Kilauea, Menengai and Krafla (Rooyakkers et al. 2021). The similarity of these eruptions suggests that mafic stratovolcanoes potentially have shallow isolated magma reservoirs, and these secondary magma chambers pose potential risks for explosive fissure eruptions.

Conclusions

We have revised the eruption sequence of Miyakejima volcano within the last ~2300 years, which spans between two caldera-forming eruptions. The revised stratigraphic framework indicates a high magma

discharge rate during the caldera-filling activity just after the Hatchodaira caldera formation, and decrease to the lateral eruption dominant period.

Temporal variations in the whole-rock of erupted magmas at Miyakejima volcano show that the activity within the last ~2300 years can be divided into three magmatic periods. Each magmatic period is characterized by the eruption of a large volume of primitive basaltic lavas at the beginning of each period, and a progressive compositional change until the end of each period. The eruption rate of magmas decreased during the last ~2300 years, from the previous caldera-formation to present.

Recharge of basaltic magma caused explosive eruptions with larger eruption volumes at the beginning of each eruption period. Another type of violent explosive eruption was fed by the rupturing of an isolated magma pocket which filled by evolved andesite magmas. Such explosive eruptions can occur not only at Miyakejima but also at other basaltic volcanoes with intermittent recharge of basaltic magmas.

Appendix

Stratigraphic analysis and ^{14}C dating

In this study, the eruption history of Miyakejima was reexamined based on the observations of the stratigraphic relationship and the ^{14}C datings in new outcrops that was formed after the 2000 AD eruption. The stratigraphic relationship of the ejecta was described at 270 outcrops throughout Miyakejima. The tephra distributing over the island (Hacchodaira volcanic ash layer, the Suoana–Kazahaya tephra, the Tenjosan tephra of the Kozushima, the Mukaiyama tephra of the Niijima, and the Sonei–bokujyo ash layer) were used for the key beds. The lithology, phenocryst abundance, and whole-rock chemical composition data of the ejecta were also used

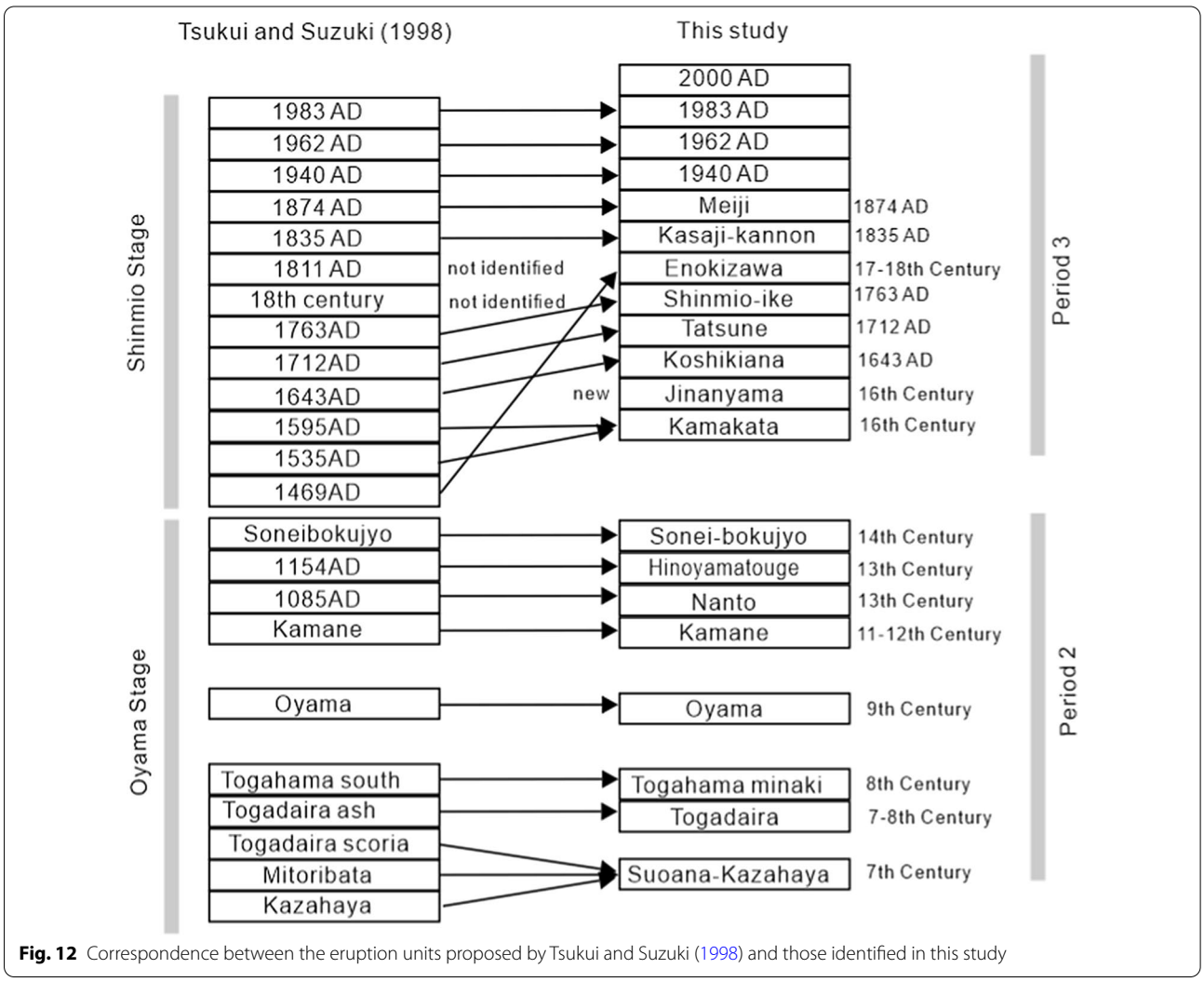

Fig. 12 Correspondence between the eruption units proposed by Tsukui and Suzuki (1998) and those identified in this study

for the identification and correlation of the deposits from different outcrops.

The chronology of the revised eruptive history is controlled by new radiocarbon ages measured for carbonized wood fragments collected inside the eruptive deposit or in the paleosol directly underlying the deposit. These samples were cleaned chemically, using acid–alkali–acid treatment, and combusted to CO_2. The purified CO_2 was then reduced to graphite. The $^{14}C/^{13}C$ ratio of the graphite was then measured using a Tandetron accelerator (NEC Pelletron 9SDH-2) mass spectrometer, at the Institute of Accelerator Analysis Ltd. The conventional ages were calibrated using the IntCal 20 program (Reimer et al. 2020).

Petrological analyses

We have undertaken petrological analyses for erupted materials from the same outcrops. Whole-rock chemical compositions were analyzed by a wavelength dispersive, X-ray fluorescence spectrometer (XRF—PANalytical Axios Advanced) in the Geological Survey of Japan (GSJ), AIST. A glass-bead method was used for the analysis of whole-rock chemical compositions. The conditions of acceleration voltage and tube current of the X-ray generator were set at 50 kV and 50 mA for detection of the Kα lines of major elements (Na, Mg, Al, Si, P, K, Ca, Ti, Mn, and Fe), 32 kV and 125 mA for Kα line of Sc, 50 kV and 80 mA for Kα lines of V and Cr, 60 kV and 66 mA for the Kα lines of Co, Ni, Cu, Zn, Rb, Sr, Y, Zr, Nb and Th, and 40 kV and 100 mA for the Lα line of Ba. A flow proportional counter was used for the elements between Na and Ti, a duplex detector system was used for Mn and Fe, and a scintillation detector for the elements larger than Co. Calibration was conducted with 12 standard reference samples (JA-1, JA-2, JA-3, JB-1a, JB-2, JB3, JG-1a, JG-2, JGb-1, JGb-2, JP-1, and JR-1) issued by the Geological Survey of Japan (GSJ). The precision (reproducibility) of analysis was evaluated with 10 repeat analyses of a glass bead of JB-1a standard. The relative standard deviations were less than 1%, for all elements. In the text and figures, we use the concentrations of each element normalized by the sum of the 10 major elements as oxide (all iron as FeO) (Fig. 12).

Abbreviations

DRE: Dense Rock Equivalent; PDC: Pyroclastic density current.

Supplementary Information

The online version contains supplementary material available at https://doi.org/10.1186/s40623-022-01577-7.

Additional file 1: Figure S1. Whole-rock concentrations of major and representative trace elements of the eruptive products of Miyakejima within the last ~ 4000 years plotted against the SiO_2 concentration.

Additional file 2: Table S1. Whole-rock chemical compositions of the eruptive products of Miyakejima within the last ~ 4000 years.

Acknowledgements

Our field survey was supported by Japan Meteorological Agency and the government of Miyake Village, and Ministry of Environment.

Authors' contributions

NG planned the framework of the study, participated in geological field surveys on the volcano, and petrological analysis and investigation of the erupted magmas. TO participated in geological field surveys on the volcano and revised the stratigraphic relationships of the deposit. DW participated in geological field surveys on the volcano and undertook petrological investigations on the erupted magmas. CC undertook petrological investigations on the erupted magmas. All authors contribute the building of the manuscript. All authors read and approved the final manuscript.

Funding

N. Geshi was supported by JSPS KAKENHI Grants 24510251 and 19K04024. C. Conway was supported by JSPS KAKENHI Grant 19K23471.

Availability of data and materials

All data generated and/or analyzed during this study are included in this published article and its Additional files.

Declarations

Competing interests

The authors declare that they have no competing interests.

Author details

[1]Geological Survey of Japan, AIST, AIST Site 7, 1-1-1 Higashi, Tsukuba, Ibaraki, Japan. [2]Earthquake Research Institute, University of Tokyo, 1-1-1 Yayoi, Bunkyo, Tokyo, Japan.

Received: 24 July 2021 Accepted: 10 January 2022
Published online: 29 January 2022

References

Amma-Miyasaka M, Nakagawa M (1998) Recent magma plumbing system beneath Miyake-jima volcano, Izu Islands, inferred from petrological study of the 1940 and 1962 EJECTA. Bull Volcanol Soc Jpn 43:433–455

Amma-Miyasaka M, Nakagawa M (2002) Origin of anorthite and olivine megacrysts in island-arc tholeiites: petrological study of 1940 and 1962 ejecta from Miyake-jima volcano, Izu-Mariana arc. J Volcanol Geotherm Res 117:263–283. https://doi.org/10.1016/S0377-0273(02)00224-X

Amma-Miyasaka M, Nakagawa M (2003) Evolution of deeper basaltic and shallower andesitic magmas during the ad 1469–1983 eruptions of Miyake-Jima Volcano, Izu–Mariana Arc: inferences from temporal variations of mineral compositions in crystal-clots. J Petrol 44:2113–2138

Amma-Miyasaka M, Nakagawa M, Nakada S (2005) Magma plumbing system of the 2000 eruption of Miyakejima volcano, Japan. Bull Volcanol 67:254–267

Endo K, Chiba T, Tanigushi H, Sumita M, Tachikawa S, Miyahara T, Uno R, Miyaji N (1988) Tephrochronological study on the 1986–1987 of Izu-Oshima volcano, Japan. Bull Volcanol Soc Jpn 33:S32–S51 (**In Japanese with English abstract**)

Ferlito C, Viccaro M, Nicotra E, Cristofolini R (2012) Regimes of magma recharge and their control on the eruptive behavior during the period 2001–2005 at Mt. Etna volcano. Bull Volcanol 74:533–543

Forni F, Degruyter W, Bachmann O, De Alis G, Mollo S (2018) Long-term magmatic evolution reveals the beginning of a new caldera cycle at Campi Flegrei. Sci Adv 4:9401. https://doi.org/10.1126/sciadv.aat9401

Fujii T, Aramaki S, Kaneko T, Ozawa K, Kawanabe Y, Fukuoka T (1988) Petrology of the lavas and ejecta of the November, 1986 eruption of Izu-Oshima volcano. Bull Volcanol Soc Jpn 33:S234–S254
Gardner JE, Carey S, Rutherford MJ, Sigurdsson H (1995) Petrologic diversity in Mount St. Helens dacites during the last 4,000 years: implications for magma mixing. Contrib Miner Petrol 119:224–238. https://doi.org/10.1007/BF00307283
Geshi N, Oikawa T (2008) Phreatomagmatic eruptions associated with the caldera collapse during the Miyakejima 2000 eruption, Japan. J Volcanol Geotherm Res 176:457–468. https://doi.org/10.1016/j.jvolgeores.2008.04.013
Geshi N, Oikawa T (2014) The spectrum of basaltic feeder systems from effusive lava eruption to explosive eruption at Miyakejima volcano, Japan. Bull Volcanol 76:797
Geshi N, Shimano T, Chiba T, Nakada S (2002) Caldera collapse during the 2000 eruption of Miyakejima volcano, Japan. Bull Volcanol 64:55–68. https://doi.org/10.1007/s00445-001-0184-z
Geshi N, Németh K, Noguchi R, Oikawa T (2019) Shift from magmatic to phreatomagmatic explosions controlled by the lateral evolution of a feeder dike in the Suoana-Kazahaya eruption, Miyakejima volcano, Japan. Earth Planet Sci Lett 511:177–189. https://doi.org/10.1016/j.epsl.2019.01.038
Isshiki N (1960) 1:50,000 Geological map of Japan, Miyake-jima with explanatory text. Geological Map 1:50,000 Geol Soc Japan 9:1–91 **(in Japanese with English abstract)**
Japan Meteorological Agency (2013) National catalogue of the active volcanoes in Japan, 4th edn. Japan Meteorological Agency, Minato City
Kamenetsky VS, Pompilio M, Métrich N, Sobolev AV, Kuzmin DV, Thomas R (2007) Arrival of extremely volatile-rich high-Mg magmas changes explosivity of Mount Etna. Geology 35:255–258
Kent AJR, Darr C, Koleszar AM, Salisbury MJ, Cooper KM (2010) Preferential eruption of andesitic magmas through recharge filtering. Nat Geosci 3:631–636. https://doi.org/10.1038/ngeo924
Kuritani T, Yokoyama T, Kobayashi K, Nakamura E (2003) Shift and rotation of composition trends by magma mixing: 1983 eruption at Miyake-jima volcano, Japan. J Petrol 44:1895–1916. https://doi.org/10.1093/petrology/egg063
Kuritani T, Yamaguchi A, Fukumitsu S, Nakagawa M, Matsumoto A, Yokoyama T (2018) Magma plumbing system at Izu-Oshima volcano, Japan: constraints from petrological and geochemical analyses. Front Earth Sci 6:1–14. https://doi.org/10.3389/feart.2018.00178
Lindsay JM, Trumbull RB, Schmitt AK, Stockli DF, Shane PA, Howe TM (2013) Volcanic stratigraphy and geochemistry of the Soufrière Volcanic Centre, Saint Lucia with implications for volcanic hazards. J Volcanol Geotherm Res 258:126–142
Luhr JF, Navarro-Ochoa C, Savov I (2010) Tephrochronology, petrology and geochemistry of Late-Holocene pyroclastic deposits from Volcán de Colima, Mexico. J Volcanol Geotherm Res 197:1–32
Matsumoto A, Nakagawa M (2010) Formation and evolution of silicic magma plumbing system: petrology of the volcanic rocks of Usu volcano, Hokkaido, Japan. J Volcanol Geotherm Res 196:185–207. https://doi.org/10.1016/j.jvolgeores.2010.07.014
Métrich N, Bertagnini A, Di Muro A (2010) Conditions of magma storage, degassing and ascent at Stromboli: new insights into the volcano plumbing system with inferences on the eruptive dynamics. J Petrol 51:603–629
Murphy MD, Sparks RSJ, Barclay J, Carroll MR, Lejeune AM, Brewer TS, Macdonald R, Black S, Young S (1998) The role of magma mixing in triggering the current eruption at the Soufriere Hills volcano, Montserrat, West Indies. Geophys Res Lett 25:3433–3436. https://doi.org/10.1029/98GL00713
Niihori K, Tsukui M, Kawanabe Y (2003) Evolution of magma and magma plumbing system of Miyakejima volcano in the last 10,000 years. Bull Volcanol Soc Jpn 48:387–405 (**In Japanese with English abstract**)
Reimer PJ, Austin WEN, Bard E, Bayliss A, Blackwell PG, Ramsey CB, Butzin M, Cheng H, Edwards RL, Friedrich M, Grootes PM, Guilderson TP, Hajdas I, Heaton TJ, Hogg AG, Hughen KA, Kromer B, Manning SW, Muscheler R, Palmer JG, Pearson C, van der Plicht J, Reimer RW, Richards DA, Scott EM, Southon JR, Turney CSM, Wacker L, Adolphi F, Büntgen U, Capano M, Fahrni SM, Fogtmann-Schulz A, Friedrich R, Köhler P, Kudsk S, Miyake F, Olsen J, Reinig F, Sakamoto M, Sookdeo A, Talamo S (2020) The IntCal20 northern hemisphere radiocarbon age calibration curve (0–55 cal kBP). Radiocarbon 62:725–757
Rooyakkers SM, Stix J, Berlo K, Petrelli M, Sigmundsson F (2021) Eruption risks from covert silicic magma bodies. Geology 49(8):921–925
Saito G, Morishita Y, Shinohara H (2010) Magma plumbing system of the 2000 eruption of Miyakejima volcano, Japan, deduced from volatile and major component contents of olivine-hosted melt inclusions. J Geophys Res Solid Earth. https://doi.org/10.1029/2010JB007433
Sumner JM (1998) Formation of clastogenic lava flows during fissure eruption and scoria cone collapse: the 1986 eruption of Izu-Oshima volcano, eastern Japan. Bull Volcanol 60:195–212. https://doi.org/10.1007/s004450050227
Suzuki Y, Tsukui M (1997) New radiocarbon dates for pyroclastics erupted from Miyakejima volcano. Bull Volcanol Soc Jpn 42:307–311 (**In Japanese**)
Tomiya A, Takahashi E (1995) Reconstruction of an evolving magma chamber beneath Usu volcano since the 1663 eruption. J Petrol 36:617–636. https://doi.org/10.1093/petrology/36.3.617
Tsukui M, Suzuki Y (1998) Eruptive history of Miyakejima volcano during the last 7000 years. Bull Volcanol Soc Jpn 43:149–166 (**In Japanese with English abstract**)
Tsukui M, Niihori K, Kawanabe Y, Suzuki Y (2001) Stratigraphy and formation of Miyakejima. Volcano J Geogr (Chigaku Zasshi) 110:156–167 (**In Japanese with English abstract**)
Tsukui M, Kawanabe Y, Niihori K (2005) Geological map of the Miyakejima volcano. Geological map of volcanoes 12. Geological Survey of Japan, AIST, Tsukuba
Ushioda M, Takahashi E, Hamada M, Suzuki T, Niihori K (2018) Evolution of magma plumbing system in Miyakejima volcano: constraints from melting experiments. J Geophys Res Solid Earth 123:8615–8636. https://doi.org/10.1029/2018JB015910
Yokoyama T, Kobayashi K, Kuritani T, Nakamura E (2003) Mantle metasomatism and rapid ascent of slab components beneath island arcs: evidence from ^{238}U–^{230}Th-^{226}Ra disequilibria of Miyakejima volcano, Izu arc, Japan. J Geophys Res 108:2329. https://doi.org/10.1029/2002JB002103
Yokoyama T, Kuritani T, Kobayashi K, Nakamura E (2006) Geochemical evolution of a shallow magma plumbing system during the last 500 years, Miyakejima volcano, Japan: constraints from ^{238}U–^{230}Th–^{226}Ra systematics. Geochi Cosmoch Act 70:2885–2901

Publisher's Note